BAND BROADENING IN SIZE EXCLUSION CHROMATOGRAPHY OF POLYMERS. STATE OF THE ART AND SOME NOVEL SOLUTIONS

J. L. Baumgarten[a]; J. -P. Busnel[b]; G. R. Meira[c]

[a] Pro Analysi, Wiehl, Germany [b] Polymères, Colloïdes, Interfaces, UMR 6120/CNRS, Université du Maine, Le Mans, France [c] INTEC (Universidad Nacional del Litoral-CONICET), Santa Fe, Argentina

PLEASE SCROLL DOWN FOR ARTICLE

BAND BROADENING IN SIZE EXCLUSION CHROMATOGRAPHY OF POLYMERS. STATE OF THE ART AND SOME NOVEL SOLUTIONS

J. L. Baumgarten,[1] J.-P. Busnel,[2] and G. R. Meira[3],*

[1]Pro Analysi, Immen 24, 51674 Wiehl, Germany
[2]Polymères, Colloïdes, Interfaces, UMR 6120/CNRS,
Université du Maine, Av. O. Messiaen 72085,
Le Mans Cedex 9, France
[3]INTEC (Universidad Nacional del Litoral-CONICET),
Guemes 3450, Santa Fe (3000), Argentina

ABSTRACT

This work reviews the main problems of band broadening (BB) in SEC, and also presents some novel and state-of-the-art solutions. The first part of the work describes Tung's equation and presents an overview on the expected order-of-magnitude of BB effects. The second part deals with the experimental determination of the broadening function using ultra-narrow standards. The third part describes several algorithms for inverting the mass chromatograms. To allow for the simultaneous occurrence of narrow and broad regions in the same chromatogram, a novel regularization filter with a position-dependent parameter was introduced. When comparing different inversion procedures, the

*Corresponding author. E-mail: gmeira@ceride.gov.ar

1967

maximum entropy method has proven effective for recuperating structural details narrower than two times the width of the kernel. For broader and smoother regions, most other inversion procedures are equally effective. The fourth part of the work aims at producing unbiased estimates in multidetection SEC. For a derived variable obtained by linear combination of two or more chromatograms, it is preferable to directly perform the calculation from the raw measurements, and then to correct the (broadened) derived variable with the standard system kernel. When estimating molar masses from in-line molar mass sensors, intolerable errors are produced near to the baselines. To cope with this problem and to simultaneously correct for BB, a theoretical procedure is reviewed that is based on recuperating the linear (unbiased) molecular weight calibration.

INTRODUCTION

Band broadening (BB) is one of several systematic effects that make difficult the data processing of SEC chromatograms. Other effects like erroneous baseline correction, false detector constants, and imprecise calibration functions can overwhelm BB. However, in many situations (and irrespective of other influences), the correction for BB is indispensable for a truly quantitative estimation.

In ideal SEC, a perfect fractionation according to hydrodynamic volume is expected. Unfortunately, perfect resolution is impossible due to secondary fractionations and to BB. Secondary fractionations result from physicochemical interactions between the polymer, the solvent, and the polymer packing,[1] and they will not be further discussed. BB is mainly due to axial dispersion in the columns, but it also includes other minor sources such as column end-fitting effects, finite injection volume, finite detection cell volume, and flow profiles in the capillaries.[2,3]

Size exclusion chromatography (SEC) is the main analytical technique for measuring the molecular weight distribution (MWD) of a polymer. BB affects the molecular weight estimates in different ways, according to the employed estimation procedure. When molar masses are indirectly estimated from an independent molecular weight calibration, and the correction for BB is neglected, the resulting MWD is broader than real and the polydispersity $\overline{M}_w/\overline{M}_n$ results overestimated. The reason is that while BB distorts the mass chromatogram, it does not affect the molecular weight calibration. To see this, assume that a calibration is carried out with strictly monodisperse standards, and that the

corresponding chromatograms are symmetrical. Then, the molecular weights are assigned at the mean elution volumes. If the same standards were reinjected, but into an ideal chromatograph without BB, then impulsive Delta functions would be expected at the same mean retention volumes. Thus, a unique calibration is obtained, irrespective of BB. Consider now the direct estimation of molar masses from in-line molar mass sensors. In this case, the resulting MWD is in general narrower than real, and the polydispersity is underestimated. To see this, assume that exact estimates of the instantaneous number-, viscosity-, and weight-average molecular weights [$M_n(V)$, $M_v(V)$, and $M_w(V)$, respectively] were obtained from ideal sensors. From $M_n(V)$, the global $\overline{M}_n$ is unbiased, while $\overline{M}_v$ and $\overline{M}_w$ are both underestimated (and therefore, the global polydispersity is again underestimated). From $M_w(V)$, the global $\overline{M}_w$ is unbiased, while $\overline{M}_n$ and $\overline{M}_v$ are both overestimated (and therefore, the global polydispersity is underestimated).[4] From $M_v(V)$, the global polydispersity can be either underestimated (if exact Mark–Houwink constants are used) or overestimated (when the universal calibration is used).[5,6]

To avoid the ill-posed nature of numerical deconvolutions, alternative procedures for producing unbiased MWDs have been developed that simply involve a rotation of the linear calibration counterclockwise around an average retention volume.[6,7] However, the correction is only exact if the following (rather strong) hypotheses are verified: (a) the MWD is log-normal; (b) the BB function is uniform and Gaussian; and (c) the molecular weight calibration $\log M(V)$ is linear. These concepts have been later extended to systems that include light scattering (LS) measurements.[8] In this case, and by using only the mid-chromatogram measurements, it is possible to simultaneously determine the slope of $\log M(V)$ and the standard deviation of the BB function.[8] In this work, none of these restrictive correction methods (from the point of view of the shapes of the MWD or the BB function) will be further discussed.

The first section of this work introduces the background of Tung's equation. The second section presents some recent results on the estimation of the elusive kernel or broadening function (BF). The third section describes a robust deconvolution procedure; and the last section discusses some novel procedures for producing more efficient deconvolutions in multidetection SEC.

GENERAL CONSIDERATIONS

Several arguments have appeared against the necessity of correcting for BB; e.g.: (i) BB is negligible in modern high-resolution columns; (ii) other sources of error (such as the baseline determination) should be preferably attacked; (iii) the broadening function is generally unknown or too difficult to obtain; (iv) numerical inversions produce infinite solutions, and many conflictive selection criteria are possible; and (v) "true" molecular weights can be measured

from molar mass sensors, and therefore the results are unaffected by BB. The previous arguments are not generally valid, however. For example, argument (i) is inapplicable when a narrow-distributed polymer is analyzed, when "sharp" details of the MWD are required, and/or when the column resolution is poor (i.e., for steep calibration curves). With reference to argument (ii), and in spite of the fact that other more important sources of error may be present, BB is unavoidable and it therefore should be always taken into consideration for truly accurate determinations. Answers to arguments (iii) to (v) are given in all that follows.

Principle of Band Formation

Tung's equation[9] was originally derived for a mass sensor, but it can be easily extended to any other detector type. To see this, note that BB mainly occurs in the fractionation columns, and this process is quite independent on the detector type. By neglecting the distortion produced in the detector cells and interdetector capillaries, it is simple to see that any generic chromatogram $s_k(V)$ is distorted by a common kernel that coincides with the standard system kernel of the mass chromatogram.

Assume that a monodisperse or uniform sample of total mass m and molecular weight M causes a detector response:[10]

$$s_k(M, V) = m \cdot g(M, V) f(M) \tag{1}$$

where V is the elution volume; $g(M, V)$ is the kernel or broadening function (BF); and $f(M)$ is the response factor or detector calibration. If now a real sample of molar mass distribution $w(M)$ is injected into a chromatograph with a calibration $M(V)$, the responses to each M add up to produce the following (noise-free) eluogram:[11,12]

$$s_k(V) = m \int_0^\infty g(M, V) f(M) w(M) \, \mathrm{d}M$$
$$= \int_{-\infty}^{+\infty} g(V, \widetilde{V}) s_k{}^c(\widetilde{V}) \, \mathrm{d}\widetilde{V} \tag{2}$$

with:

$$s_k{}^c(V) = mf(V) u(V) \qquad \text{(``corrected'' or sharp response)} \tag{3}$$

$$u(V) = w(M(V)) \left(\frac{\partial M(V)}{\partial V} \right) \qquad \text{(normalized sharp response)} \tag{4}$$

where $\widetilde{V}$ represents the average retention volume of an hypothetical monodisperse sample.

From $u(V)$, the average molecular weight averages and other derived variables may be calculated (Table 1).

Order of Magnitude of the Band Broadening Effects

Without BB correction, $s(V)$ is used instead of $s_k^c(V)$. To explore the magnitude of this effect, we first examine a purely analytical model with the following properties:[13–17] (i) a chromatographically-simple polymer has a sharp normalized eluogram $u(V)$, that is Gaussian-shaped of average V_0 and variance σ_u^2; (ii) the kernel g is uniform (or position-independent), and Gaussian of variance σ_g^2; and (iii) the calibration function is linear, i.e.:

$$\log[M(V)] = A - BV \tag{5}$$

The broadened "measurements" from a differential refractometer (DR), a light scattering (LS) sensor or an intrinsic viscometer (IV) (s_{DR}, s_{LS}, and s_{IV}, respectively) can be calculated by inserting Eqs. (3) and (4) into Eq. (2). It turns out, that all of these "chromatograms" are also Gaussian. The ratios s_{LS}/s_{DR} or s_{IV}/s_{DR} can be interpreted as calibrations obtained from the LS and IV signals. These ad hoc calibrations are only valid for the analysed sample, and adopt the same form of Eq. (5), but with different coefficients, i.e.:

$$\log(s_k/s_{DR}) = A_k - B_k V \qquad (k = \text{LS or IV}) \tag{6}$$

When using either the conventional linear calibration of Eq. (5), or Eq. (6) for a LS sensor, we can plot the ratio between the estimated and the true nonuniformity U vs. σ_u^2/σ_g^2, where σ_u^2 has been varied in a wide range of values (see abscissa of Fig. 1). Call $\hat{U}_{DR}$ and $\hat{U}_{LS/DR}$ the estimates of U respectively obtained from the ideal DR signal + the conventional calibration, and from the ideal LS + DR sensors. When σ_u^2 becomes close to or smaller than σ_g^2, then $\hat{U}_{LS/DR}$ results underestimated while $\hat{U}_{DR}$ results overestimated. Figure 1 also shows that (for a linear calibration with ideal DR and LS measurements), the

Table 1. Basic Definitions

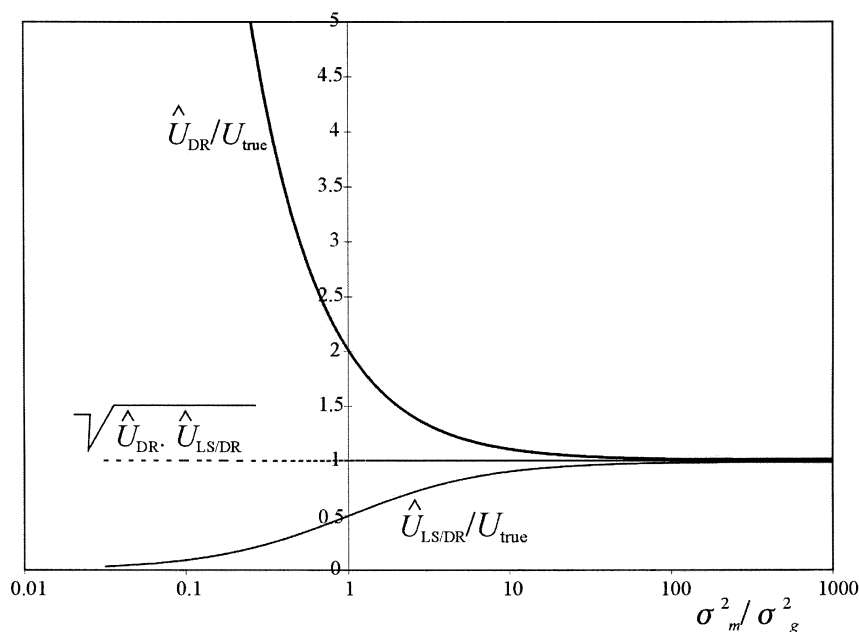| Expression	Name
$\langle M^L \rangle = \int M^L(V)\,u(V)\,\mathrm{d}V$	L-th moment
$\overline{M}_J = \langle M^{J-1} \rangle / \langle M^{J-2} \rangle$	$\overline{M}_n$ for $J = 1$, $\overline{M}_w$ for $J = 2$, $\overline{M}_z$ for $J = 3$
$D = \overline{M}_w / \overline{M}_n$	Polydispersity or polymolecularity index
$U = D - 1$	Nonuniformity index or nonuniformity

Figure 1. The effect of BB on the nonuniformity U is numerically investigated assuming both a conventional linear calibration and an ideal LS-DR calibration. The numerical example assumes a series of Gaussian "chromatograms" of mean retention volume 30 mL and varying variances. The kernel is uniform and Gaussian, with a fixed variance $\sigma_g^2 = 0.18034$ mL^2. The abscissas are the ratio between the variance of the true sharp response and the variance of the kernel. The ordinates represent the ratio between the estimated U and the true U. The linear calibration is defined by $M\,(20\,\text{mL}) = 10^6$ g/mol and $M\,(40\,\text{mL}) = 10^4$ g/mol. Three estimates of U are compared: (1) $\hat{U}_{\text{DR}}$ was obtained by combining the DR signal with the conventional calibration; (2) $\hat{U}_{\text{LS/DR}}$ corresponds to an ideal LS-DR calibration; and (3) the horizontal line was obtained by averaging the two previous estimates.

sample nonuniformity can be accurately calculated through the following average of the previous estimates:

$$U_{\text{true}} \approx \sqrt{\hat{U}_{\text{DR}}\hat{U}_{\text{LS/DR}}}$$

Similarly, from the ad hoc calibration $s_{\text{IV}}/s_{\text{DR}}$, we can retrieve the intrinsic viscosity or Staudinger index $[\eta]$, and evaluate the deviation of the Mark–Houwink parameters a and K, when either the conventional or the LS calibrations

are used. With the conventional calibration, the estimates $\hat{a}_{DR}$ and $\hat{K}_{DR}$ are considerably deteriorated (Fig. 2). With the LS calibration, the errors are lower than 0.1% for, and almost 0% for $\hat{a}_{LS}$. The following comments can be made.

Irrespective of the applied calibration procedure, the errors in the average molecular weights are generally lower than 10%.

With the conventional calibration, the estimates $\hat{U}_{DR}$, $\hat{K}_{DR}$, and $\hat{a}_{DR}$ are all significantly affected; in particular when the sample variance is an order of magnitude lower than the kernel variance.

With the LS calibration, only $\hat{U}_{LS/DR}$ remains sensitive, but the errors are very low for narrow samples, while the misleads in $\hat{K}_{LS}$ and $\hat{a}_{LS}$ are below *ca.* 0.3%.

An extension to $U_{true} \approx \sqrt{\hat{U}_{DR}\hat{U}_{LS/DR}}$ is given later by Eq. (14), that is valid for arbitrary shapes of the kernel and the eluogram.
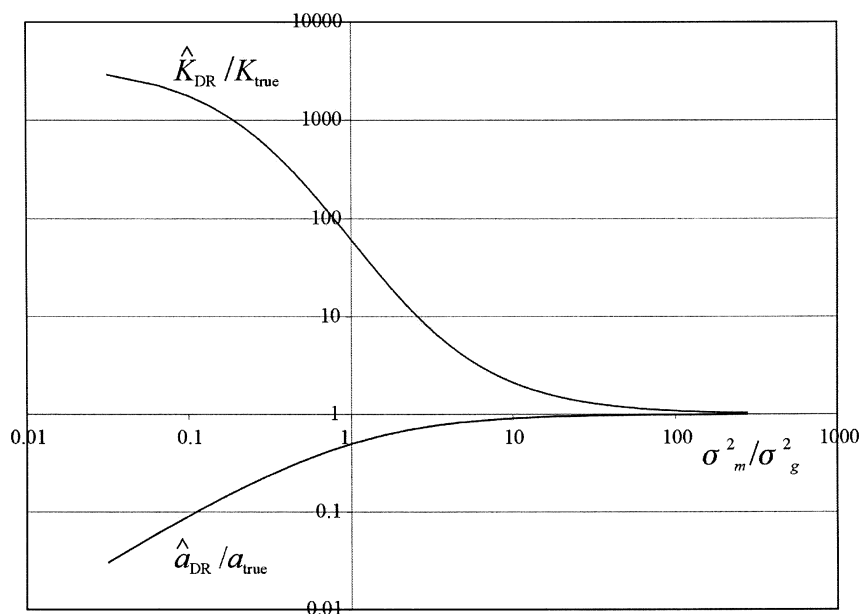
Figure 2. The numerical example of Fig. 1 is here reconsidered, but assuming that the true global [η] is known from ideal DR and IV signals; and that the corresponding Mark–Houwink are estimated from the DR signal + the conventional calibration. The ratio of the estimated over the true K and a parameters (in logarithmic scale) is represented vs. the ratio between the variance of the true sharp response and the variance of the kernel.

BAND BROADENING FUNCTION

A key aspect of BB correction is to establish the precise broadening function (BF) for the specific chromatographic system.

The first attempts of BB correction were focused on improving the inversion methods, while the BF was assumed Gaussian (either with a constant or variable variance σ_g^2). The following experimental methods have been tested.

Direct comparison between the polydispersities (or polymolecularity indexes) $\overline{M}_w/\overline{M}_n$ obtained by SEC integration and by absolute average molecular weight measurements. For broad-distributed samples, the kernel was assumed uniform and Gaussian. For a set of narrow standards, the local values of σ_g^2 could be estimated.[14]

Reverse flow technique. It consists of analysing a narrow standard and to reverse the flow just before the beginning of its elution. In this way, the polymolecularity effect is compensated, and the width of the chromatogram is an indication of σ_g.[9,18]

For a broad-distributed sample, one can compare the ad hoc calibration $M_w(V)$ obtained from a LS sensor $M_w(V)$ with an independent calibration $M(V)$ obtained with narrow samples $M(V)$.[19]

An important state-of-the-art review has been published by Hamielec in 1984.[12] In all his treatments, the BF was assumed Gaussian. This involved a simplification of the necessary data treatment, as required by the limited computing facilities of that time. Later, the same general ideas were adapted and improved by other authors,[20–22] but always maintaining the Gaussian assumption.

At present, SEC column performance has strongly improved, and also a precise examination of the peak shapes from almost monodisperse samples is possible. Very narrow and low-molecular-weight samples clearly indicates that peaks are always skewed, thus, making the Gaussian assumption unrealistic.

Attempts to define the BF from strictly theoretical considerations are so far impossible. The reason is, that not only many parameters affect the broadening in the column, but also a broadening is produced in the interconnecting tubes and detectors. However, the theoretical interpretation is still useful to decide the directions of future improvements.

Direct examination of peak shape from narrow polymer standards does not provide useful information on the BF, since their peak shape results from a combination of BB and polymolecularity. Finally, and just for citation, attempts have been made to estimate the BF by examination of chromatograms from broad-distributed samples. However, in this case, only averaged BB effects can be determined.

Ultra Narrow Sample Analysis

At present, the best estimations of the BF are obtained by direct observation of ultra-narrow polymer samples, with polymolecularities that negligibly affect the peak shape.

Thermal Gradient Interaction Chromatography (TGIC) exhibits a better resolution than SEC for analyzing narrow and linear PS samples prepared by anionic polymerisation with careful deactivation of the chain ends. Thus, preparative TGIC allows isolation of ultra-narrow PS fractions with polymolecularities lower than 1.005.[23–25] We have recently analysed such ultra-narrow samples on three column sets of different fractionation ranges, to determine their BFs.[26] Peak shapes confirm that skewing occurs systematically. With an excellent correlation coefficient (see Fig. 3), these peaks can be fitted with either exponentially-modified Gaussians[27] (EMG) or exponential-Gaussian hybrid functions[28] (EGH). In both cases, a Gaussian dispersion characterised by σ_x^2 is combined with an exponential decay characterised by τ_g. Consider the expressions for σ_g^2 and τ_g presented in Table 2. For low- or medium-molecular weights, both

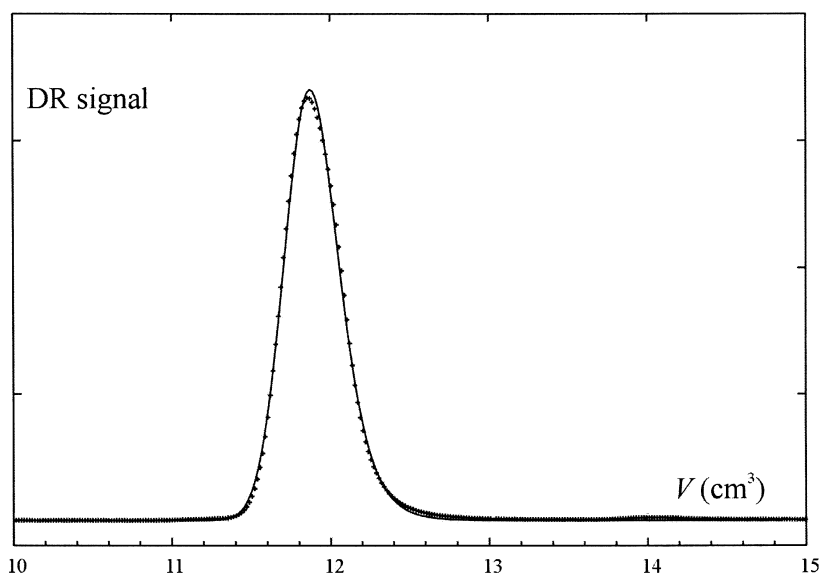*Figure 3.* The chromatogram of an ultra-narrow PS sample (continuous line) is fit to an exponentially-modified Gaussian function (dotted line). The sample exhibits a molar mass of 384,000 g/mol and a polymolecularity index of 1.004. The analysis was carried out using a 60 cm column from Polymer Labs (gel mixed C). The parameters of the EMG fit are: $\sigma_g = 0.146\,cm^3$; $\tau_g = 0.124\,cm^3$; and $R^2 = 0.999$.

Table 2. Nonuniform Broadening Functions for Three Commercial Column Sets: Variation of the EMG Parameters

Column Set	Jordi^{TM} 100 Å(50 cm)	Pol. Lab.^{TM} Mixed C (60 cm)	Pol. Lab.^{TM} Mixed B (260 cm)
Zone of feasible BB correction			
MW range (g/mol)	60,000–500	600,000–500	2×10^6–15,000
V range (cm^3)	14–23	11–19	21–30
σ_g (cm^3)	$0.159 - 0.001\ V$	$0.165 - 0.002\ V$	$0.46 - 0.008\ V$
τ_g (cm^3)	$0.130 - 0.0005\ V$	$0.160 - 0.0015\ V$	$0.25 - 0.005\ V$
Zone near total exclusion volume			
V range (cm^3)	12–14	10–11	19–21
σ_g (cm^3)	0.09–0.1	0.15–0.16	0.2–0.25
τ_g (cm^3)	0.2–0.3	0.2–0.45	0.4–0.5

parameters are quite independent of elution volume as long as we stay away from total exclusion. However, close to total exclusion, a great increase in peak skewing is observed. For high molecular weight polymers, a more pronounced increase in peak width and skewing with molecular weight is observed, and again a strong increase in the skewing is seen near total exclusion.

A precise correction for BB needs to take into account the nonuniformity and the skewed characteristic of the BF. A convenient way of defining the kernel matrix is to represent the BF with a nonuniform EMG or EGH function, with the functions $\sigma_g^2(V)$ and $\tau_g(V)$ smoothened from the set of experimental data.

Serious difficulties appear when part of the sample elutes near total exclusion. In this case, an important peak-tailing is observed and the pollution extends quite beyond total exclusion. In this case, peak fitting by EMG or EGH becomes complicated, and the BB correction does not provide useful results.

Stability of the Broadening Function

To be useful, BB correction must be applicable in a variety of situations, and this requires a reasonable stability of the BF. Our experiments with ultra-narrow samples have clearly indicated that the BF must be established for each column set and for each running condition. In effect, the BF is significantly affected when changing the flow rate, the column volumes, or the injected volume. Fortunately, SEC analyses are generally run under quite constant conditions.

An additional constraint is the necessary prevention of overloading. This effect is even observed with narrow commercial standards; and occurs when the

viscosity of the injected solution is significantly higher than the solvent viscosity. In this case, both the peak width and the peak position change with the injected concentration.[29] As a rule of thumb, the "concentration effect" is negligible when the specific viscosity is lower than 0.1. However, for a really good BF stability, it is preferable to maintain the specific viscosity under 0.05.

Spectacular changes in peak shape also occur when adsorption effects are in competition with pure steric exclusion. This can be observed in THF solutions of poly(ethylene oxide) (PEO) or copolymers with grafted PEO.[30] In the presence of a reversible adsorption, both peak shape and peak position are affected even in dilute solution. Thus, no general BF correction can be attempted in this case.

Reinjection of Narrow Fractions Isolated from a
Broad-Distributed Sample

For many polymer architectures or chemical compositions, it is quite difficult to obtain the corresponding ultra-narrow samples. In these cases, the following versatile (but indirect) method can be attempted. For a given apparatus and running conditions, we first analyze a broad MWD sample. Then, we collect sharp fractions of the original sample, and reinject these fractions. The chromatograms of the reinjected fractions are strongly dependent on the BF. Thus, a single broad MWD sample can provide useful information on the BF in a wide elution volume range. An important requirement is to prevent any overloading during the first analysis. The extremely low concentrations of the reinjected samples require high detector sensitivity for producing acceptable chromatograms.

The peak shape of a reinjected fraction depends on both the BF and the fraction concentration. For this reason, we need to interpret the results indirectly. In a first stage, an initial BF is used to correct the broad MWD chromatogram for BB. This yields the true weight fraction distribution of the original sample and of any fraction collected in a well-defined elution volume segment. In a second stage, the same BF set is used to predict the chromatogram shapes of each fraction; and the prediction is then compared with the measurements (Fig. 4). This indirect method is valuable to check if the BF directly established from ultra-narrow PS samples appropriately predicts the shape of reinjected fractions of a different polymer. For a given apparatus, it is less secure to establish the BF ab initio, by trial and error.

The method was first tested using a broad-distributed polystyrene, and an excellent fit was obtained. This preliminary test allowed verifying the routines and to confirm the basic assumption by which the chromatogram of a complex sample is obtained, by simple addition of its different intervening species. Three polymers of quite different architectures have been tested. Two of the samples
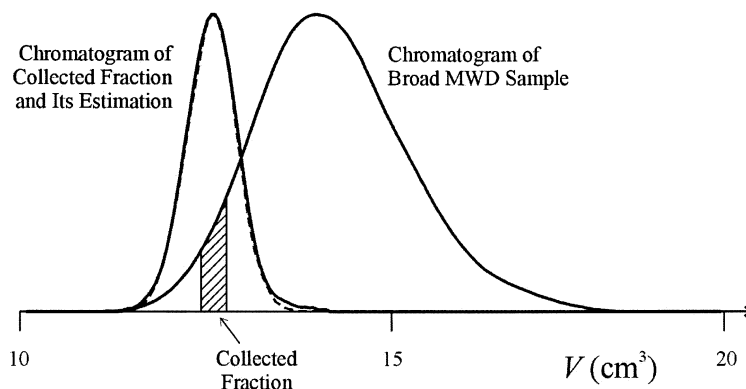
Figure 4. Recuperation of an ultra-narrow fraction from a broad MWD sample of poly(octadecyl acrylate); and fit of the chromatogram produced by such ultra-narrow fraction. The fit of the narrow chromatogram was produced from an (a priori determined) broadening function.

were comb-like polymers [a poly(octadecyl acrylate) and a poly(lauryl methacrylate)]. The third sample was a highly branched polyurethane, synthesised by reaction between 1,6-diisocyanatehexane and polyoxypropylene triol with stoichiometry –NCO/–OH = 0.54. In all three cases, the quality of the fits were similar to those obtained with PS.

In summary, for SEC run with THF under conditions of pure steric exclusion without overloading, the BF is stable for a given elution volume range and apparatus.

Water-Soluble Polymers

For water-soluble polymers, the situation is more complex than for polymers that are soluble in organic solvents. Column efficiency is often limited, and this increases the importance of BB correction. Also, adsorption effects tend to compete with steric exclusion, and it is important to verify the stability of the BF. For a rapid estimation of the BF, the simplest starting point is the direct use of the peak shape of a pure low-molecular weight sample or a pure protein. The architecture of globular proteins is quite different from the architecture of linear polymers, and for the former, there is no direct evidence of a proper BF stability. For a more careful examination of a sample or family of samples, the estimation of the BF by iterative reinjection of narrow fractions is feasible, but highly time-consuming.

NUMERICAL INVERSION

In Section 1, we have used a simple model to calculate the order of magnitude of the errors produced when a broadened $s_k(V)$ is used, instead of the sharp $s_k^c(V)$. Now, we turn to methods for correcting this misleading point for single eluograms.

Calculation of Unbiased Average Molecular Weights

There are two basic methods for retrieving the average molecular weights from a mass chromatogram and a conventional calibration. In Method 1, one first calculates the averages from the raw data, and then applies the universal correction factors (see next section). In Method two, one first deconvolutes the raw chromatogram and then calculates the quality parameters. Finally, an alternative procedure involving the use of ideal LS sensors will be considered.

For in-line molar mass detection through LS or IV sensors, only Method 2 is, in principle, applicable. However, additional strategies can be used in combination with Method 2; and these strategies are described in Section 4.

Hamielec[13] showed that for arbitrary-shaped eluograms and the following conditions:

(a) $g\left(V, \widetilde{V}\right) = g\left(V - \widetilde{V}\right)$ (the BF is uniform); and   (7)

(b) $\dfrac{M(V)}{f(V)} = \exp(A' - B'V)$ (the calibration is linear)   (8)

any (biased) average molecular weight $\overline{M}_{J,s}$ retrieved from a band-broadened mass chromatogram may be converted into the corresponding true average $\overline{M}_{J,u}$ through:

$$\overline{M}_{J,u} = F_J(g)\overline{M}_{J,s} \tag{9}$$

with

$$F_J = \frac{\Lambda(g, (J-1)B')}{\Lambda(g, (J-2)B')} \tag{10}$$

where F_J (with $J = 1$ for $\overline{M}_n$, and $J = 2$ for $\overline{M}_w$) is the so-called universal factor; and Λ indicates a Laplace transform. In particular, for Gaussian kernels, Eq. (10) results:

$$F_J = \exp\left[-\left(J - \frac{3}{2}\right)\sigma_g{}^2 B'^2\right] \tag{11}$$

For skewed kernels, other expressions have been developed.[31]

Consider, in what follows, a novel method for producing unbiased $\overline{M}_n$'s. More specifically, for systems with uniform kernels, linear calibrations, and ideal DR and LS sensors, it is possible to correct the biased average molecular weight without any a priori knowledge of the kernel shape.[17] Assume, for example, that the global $\overline{M}_w$ obtained from a LS-calibration is exact (i.e.: $\overline{M}_{w,u} = \overline{M}_{w,\text{LS}}$). Then, if the true nonuniformity U_u were known, then the corrected $\overline{M}_n$ results:

$$\overline{M}_{n,u} = \frac{\overline{M}_{w,\text{LS}}}{1 + U_u} \tag{12}$$

Through a Monte-Carlo-study, it has been shown,[17] that irrespective of the shapes of eluogram and kernel, the following expression can be used to estimate U_u, with relative error lower than 10% for narrow samples, and lower than 0.1% for broad samples:

$$U_u \approx U_{\text{corr}} = \sqrt{\left(\frac{\overline{M}_{w,\text{LS}}}{\overline{M}_{n,\text{LS}}} - 1\right)\left(\frac{\overline{M}_{w,\text{DR}}}{\overline{M}_{n,\text{DR}}} - 1\right)} \tag{13}$$

Inserting Eq. (13) into Eq. (12), one obtains:

$$\overline{M}_{n,u} \approx \overline{M}_{n,\text{corr}} = \frac{\overline{M}_{w,\text{LS}}}{1 + \sqrt{(\overline{M}_{w,\text{LS}}/\overline{M}_{n,\text{LS}} - 1)(\overline{M}_{w,\text{DR}}/\overline{M}_{n,\text{DR}} - 1)}} \tag{14}$$

Assuming a low-resolution column, Fig. 7 compares the relative errors of the following average molecular weights: $\overline{M}_{n,\text{DR}}$ (calculated from the DR signal + the conventional calibration), $\overline{M}_{n,\text{LS}}$ (calculated from ideal DR and LS signals), and $\overline{M}_{n,\text{corr}}$ [calculated using Eq. (14)]. In the simulated example, a uniform but skewed kernel was assumed and many arbitrary eluograms were investigated. Such eluograms were obtained by first adding up to four Gaussians, and then convoluting the result with an EMG kernel. The following can be observed in Fig. 5: (1) the errors in $\overline{M}_{n,\text{DR}}$ are quite large and evenly spread in the investigated region; (2) the errors in $\overline{M}_{n,\text{LS}}$ are relatively lower, but as expected, they are all in excess; and (3) the relative errors obtained through Eq. (14) $\overline{M}_{n,\text{corr}}$ are all below 0.001.

Full Inversion of Tung's Equation

Hamielec's correction factors are inapplicable for LS and IV detection. Full BB correction allows obtaining not only the true global averages, but also subtle MWD details like multimodes or hidden oligomer peaks. However, this "ill-posed" problem[32] requires sophisticated inversion tools for reasonable solutions.
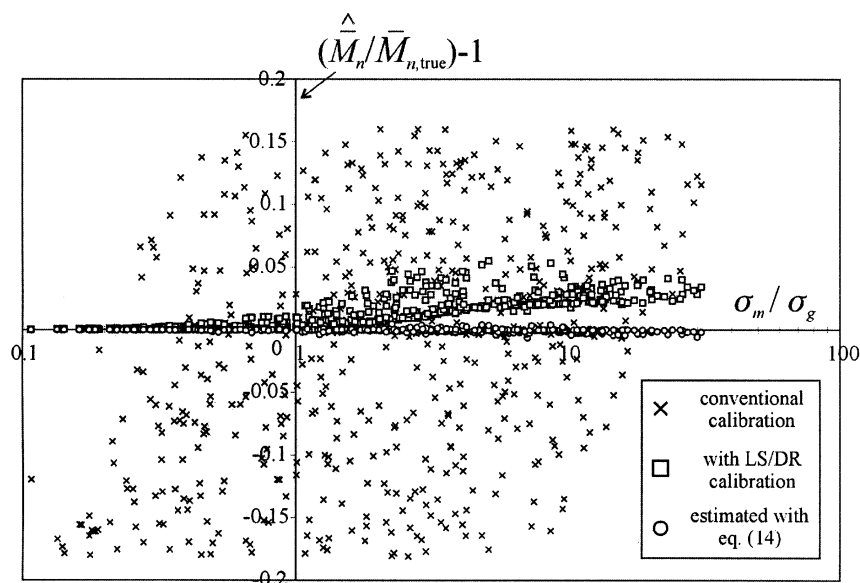
Figure 5.   Results of a Monte-Carlo study that investigates the effectiveness of Eq. (14) for estimating the global $\overline{M}_n$ from ideal DR and LS signals, assuming that the molecular weight calibration is linear and that the kernel is uniform but arbitrary. The log-linear calibration function has the following edge-points: $M(20\,\text{mL}) = 10^6\,\text{g/mol}$, and $M(40\,\text{mL}) = 10^3\,\text{g/mol}$. Many arbitrary eluograms were composed by summing up to four Gaussians (positioned close to each other) and convolving the result with an EMG-kernel of half-width 1 mL and τ_g in the range $[-0.5\,\text{mL}\text{–}0.5\,\text{mL}]$. Stochastically-chosen eluograms have shapes varying from pure Gaussian to skewed shapes and multimodal compositions. The abscissa is the ratio between the standard deviation of the sharp eluogram and the standard deviation of the kernel. The ordinate represents the relative errors of $\overline{M}_n$, according to the following calculation methods: (a) using the conventional calibration (crosses); (b) from ideal LS measurements (squares); and (c) by application of Eq. (14) (circles).

Mathematically speaking, Eq. (2) is an inhomogeneous Fredholm integral of first kind.[33] To find $\mathbf{s_k}^c(\mathbf{v})$ by numerical methods, Eq. (2) can be approximated by discretization of $\widetilde{V}$ into small $\Delta\widetilde{V}$-steps, yielding:

$$\mathbf{g} \times \mathbf{x} \approx \mathbf{y} = \mathbf{s} + \mathbf{v} \tag{15}$$

where $\mathbf{g}$ is the kernel matrix; $\mathbf{y}$ is the measured vector; $\mathbf{x}$ is the searched vector; $\mathbf{s}$ is the noise-free signal at discrete positions V_n; and $\mathbf{v}$ is a zero-mean additive measurement noise of variance σ_v^2.

The sought $\mathbf{x}$ should be as close to $\mathbf{s_k^c}$ as possible. In Eq. (15), an "approximately equal sign" is included because when directly solving $\mathbf{g} \times \mathbf{x} = \mathbf{y}$, we get:

$$\mathbf{x} = \mathbf{g}^{-1} \times \mathbf{s} + \mathbf{g}^{-1} \times \mathbf{v} \tag{16}$$

Unfortunately, $\mathbf{g}^{-1} \times \mathbf{v}$ is dramatically oscillating for Fredholm integrals, and often its magnitude is larger than that searched solution $\mathbf{s_k^c}$. This extreme sensitivity to noise is known as "ill-posedness".

We want to find a useful solution, $\mathbf{x}$, such that the model $\mathbf{m} = \mathbf{g} \times \mathbf{x}$ is as close as possible to $\mathbf{s}$; i.e.:

$$\sum_{n=1}^{N} (\mathbf{g} \times \mathbf{x} - \mathbf{s})_n^2 = \text{Min}(\mathbf{x})! \tag{17}$$

If such a solution were found, then the following is expected:

$$\frac{1}{N} \sum_{n=1}^{N} [\mathbf{g} \times \mathbf{x} - (\mathbf{s} + \mathbf{v})]_n^2 = \sigma_v^2 \tag{18}$$

Thus, the idea is not minimizing the residuals of m and $\mathbf{y}$, but rather keeping them close to the statistical noise σ_v^2. Equation (18) is a single equation with N unknowns. Then, infinite solutions can fulfil it, and the problem cannot be solved unless additional information is provided on the expected solution. A serious data analysis never freely invents information. The following conditions can be imposed onto the expected solution: (1) boundary condition: for physical reasons, the solution must be nonnegative; i.e.: $x_n > 0$ for all n; and (2) informativity conditions: information is a matter of definition, and a variety of possibilities are presented in what follows. The problem is to find a unique solution to Eq. (18) with a minimal of information.

Inversion Methods

Numerous inversion methods have been proposed. Van Cittert[34] iterates a solution to the "wrong" Eq. (15), which is stopped when Eq. (18) is verified. This method was independently reinvented for SEC applications by Chang and Huang[35] and by Smit,[36] as continuum versions of the Schulz and Hotelling method for the general iterative matrix inversion.[37] In the Quadratic Regularization by Tikhonov[32] and the Singular Value Filtering[38] (SVF), smoothness criteria with adaptive parameters are defined that match Eq. (18). Jansson et al.[39] generalize the van Cittert[34] boundary conditions imposing: $x_{\min_n} \leq x_n \leq x_{\max_n}$. The Linear Optimization Method[40] produces the same settings as the Jansson-van Cittert method; and both techniques solve a quadratic regularization problem

for the mentioned boundary conditions. The Maximum Entropy Method[41] (MEM) is a highly nonlinear regularization method, specifically designed for high-resolution tasks. Other inversion methods are given in Schell,[42] Biraud,[43] Ishige,[44] Backus–Gilbert,[45] and Essenreiter.[46]

In the following, we shall concentrate on the most widely-used, best-defined, and simplest of methods: SVF and quadratic regularization (including MEM). The regularization method will be presented in a new generalized fashion.

Regularization

Call Q a measure of "informativity". Some frequently-used information filters are listed in Table 3. Then, a solution $\mathbf{x}$ can be found such that:[32,33,41,47]

$$\chi^2(\mathbf{x}) = \sum_{n=1}^{N} (\mathbf{g} \times \mathbf{x} - \mathbf{y})_n{}^2 + \lambda Q(\mathbf{x}) = \mathrm{Min}(\mathbf{x}) \tag{19}$$

where $\chi^2(\mathbf{x})$ is the objective function to be minimized; and λ is an adjustable parameter that must be selected to fulfil Eq. (18). (A large λ puts more preference to the a priori information Q, while a small λ puts more weight on the measurements.)

Singular Value Filtering (SVF)

Like in regularization, SVF[38,48] acts as a smoothing- (or low-pass-) filter. When solving Eq. (15) in the manner of the least squares, the following analytical result is obtained:

$$\mathbf{g}^T \mathbf{g} \times \mathbf{x} = \mathbf{g}^T \times \mathbf{y} \tag{20}$$

A Singular Value Decomposition (SVD) is performed when matrix $\mathbf{g}^T\mathbf{g}$ is expressed as follows:

$$\mathbf{g}^T \mathbf{g} = \mathbf{V} \times \mathbf{D} \times \mathbf{V}^T, \tag{21}$$

where $\mathbf{V}$ is the orthogonal right eigenmatrix of $\mathbf{g}^T\mathbf{g}$; and $\mathbf{D}$ is the diagonal matrix of the $d_j{}^2$ eigenvalues of $\mathbf{g}^T\mathbf{g}$; i.e.: $[\mathbf{D} = \mathrm{diag}(d_j{}^2)]$.

In contrast, a Singular Value Filtering (SVF) involves inserting Eq. (21) into Eq. (20) and then applying the weights Φ_j onto all $1/d_j{}^2$'s, resulting:

$$\mathbf{x} = \mathbf{V} \times \mathrm{diag}\left(\frac{\Phi_j}{d_j{}^2}\right) \times \mathbf{V}^T \times \mathbf{g}^T \mathbf{y} \tag{22}$$

Some frequently used Singular Value Filters are shown in Table 4.

Table 3. Frequently-Used Regularization Filters

Formulae	Name	Comment
$Q_{\text{REG0}} = \sum\limits_{n=1}^{N} x_n{}^2$	Zero order regularization (REG0)	Keeps all x-component close to zero. Smoothing strength close to t-axis is weaker than far from it.
$Q_{\text{REG2}} = \sum\limits_{n=1}^{N} (2x_n - x_{n-1} - x_{n+1})^2$	Second order regularization (REG2)	Keeps x being a straight line. Smoothing strength is independent of value.
$Q_{\text{MEM}} = \sum\limits_{n=1}^{N} (ax_n)\ln(ax_n)$	Maximum entropy method (MEM)	Keeps x nonnegative. Smoothing strength close to t-axis is stronger than far from t-axis.

Filter Adjustment

All filters contain parameters that must be adjusted to the given data and noise. To this effect, any of the following three methods can be applied.

The Noise Adaption Method[49] (NAM) has already been introduced through Eq. (19); and it requires the residuals of measurement and model to match the variance of the statistical noise.

Table 4. Some Frequently-Used Singular Value Filters

Filter Φ_j	Name	Comment
1	Nonfiltered solution	This is the useless direct solution to Eq. (12).
$\begin{cases} 0, & \text{if } d_j{}^2 < d_{\text{Min}} \\ 1, & \text{if } d_j{}^2 \geq d_{\text{Min}} \end{cases}$	Heavyside filter	In practice (with typical SEC kernels), smooth eigenvectors have large eigenvalues, while oscillating eigenvectors have small eigenvalues.
$d_j{}^2/(d_j{}^2 + \lambda)$	Zero-order regularization	Analytical solution of Eq. (16) with REG0. SVF and regularization overlap at this point.

BAND BROADENING IN SIZE EXCLUSION CHROMATOGRAPHY   **1985**

The Optimal Wiener Filter[50] (OWF) is defined as follows. First, imagine that the true solution to $\mathbf{x}$, $\mathbf{s_k}^{\mathbf{c}}$, were known. Then, for any filter with parameters $\{\lambda_1, \ldots, \lambda_j\}$, optimize those parameters such that:

$$\langle (\mathbf{x} - \mathbf{s_k}^{\mathbf{c}})^2 \rangle = \text{Min!} \tag{23}$$

where the averaging brackets are taken over all possible realizations of the statistical noise. Unfortunately, the OWF is not directly available from the original data.

The Self Consistent Filter Optimization[47] (SCFO) compensates the unavailability of the OWF through the following approximation. Imagine that for any given λ_1, a regularization equation has the solution $\mathbf{x_1} = \mathbf{x}(\lambda_1)$. Then, the following procedure must be carried out:

> Form the model $\boldsymbol{m_1} = \mathbf{g} \times \mathbf{x_1}$, and add noise to $\mathbf{m_1}$; and
>
> Deconvolve m_1 with a different λ_2 to find:
> $$\langle (\mathbf{x_2} - \mathbf{x_1})^2 \rangle|_{\lambda_1 = \lambda_2} = \text{Min!} \tag{24}$$

Monte Carlo simulations[47] for a zero-order regularization showed that (compared with NAM), SCFO generally leads to a λ value that is closer to the optimal Wiener value.

Localized Regularization

When deconvoluting "peaky" data, the optimal λ must be small, whereas for smooth data it must be large. If a single eluogram contains both peaky and smooth data, then λ must be position-dependent. This can be expressed as follows:

$$\chi^2(\mathbf{x}) = \sum_{n=1}^{N} (\mathbf{g} \times \mathbf{x} - \mathbf{y})_n^2 + \sum_{n=1}^{N} \lambda(n, p_1, \ldots, p_J) q(x_n) = \text{Min!} \tag{25}$$

where now λ is position-dependent, since it depends on J independent p_j parameters. To adjust these parameters, we can generalize the SCFO method to the multi-parameter-form, requiring:

$$\langle (\mathbf{x_2} - \mathbf{x_1})^2 \rangle|_{p_{J,1} = p_{J,2}} = \text{Min!} \quad \text{(for all } j\text{).} \tag{26}$$

Equation (26) is possibly the most reliable method, in spite of the fact that a numerical iteration is required. In modern personal computers (and even for the highly nonlinear and nonlocal MEM), the calculation time for 1024 data points is around 1 s.

Inverting Tung's Equation for Nonlinear Detector Response

Response coefficients may depend on the absolute concentration, and this can become a severe problem for the higher molecular weights. The problem is solved through the following (rather fast) iterative procedure: (1) invert the equation with infinite-dilution-information, leading to a solution $\mathbf{x}(1)$; and (2) repeat using $\mathbf{x}(n-1)$ values to get solutions $\mathbf{x}(n)$ until convergence. Only for extremely narrow samples, does this procedure require more than two or three iterations.

Comparison and Use of Inversion Methods

In the past, the use of especial inversion algorithms was restricted by computer space and time. At present, 100 nonlinear iterations involving thousands of data points can be completed within seconds. However, not every problem requires the highest possible sophistication.

Figure 6 compares the performance of three quadratic filters (SVF, REG0, and REG2) with the MEM filter, for a series of Gaussian chromatograms with an increasing half-width. While the solutions from all quadratic filters are almost coincident, the MEM filter seems preferable for the very narrow samples.

In Fig. 7, an oligomer is resolved by local REG2, local MEM, and global MEM. Again, narrow structures were only efficiently solved by MEM. The difference between the local and global filters is less pronounced. The MEM solutions do not exhibit artificial side-lobes. Also, the broad region is deconvoluted into a single smooth solution, and all peaks in the oligomer region are resolved down to the baseline.

DERIVED VARIABLES IN MULTIDETECTION SEC

Linear vs. Nonlinear Signal Processing

In multidetection SEC, two or more detectors are installed in series. This introduces the interdetector volume problem, by which a downstream signal may be shifted and distorted with respect to an upstream signal.[3,5,21,22,51,52] This problem is neglected in the discussion that follows.

Figure 8 illustrates a case of multidetection SEC. The chromatograph is fit with a UV absorbance sensor at two different wavelengths (UV1 and UV2), a LS sensor, a capillary IV, a (hypothetical) colligative property osmometer (OS), and a DR. The corresponding signals are $s_{UV1}(V)$, $s_{UV2}(V)$, $s_{LS}(V)$, $s_{IV}(V)$, $s_{OS}(V)$, and
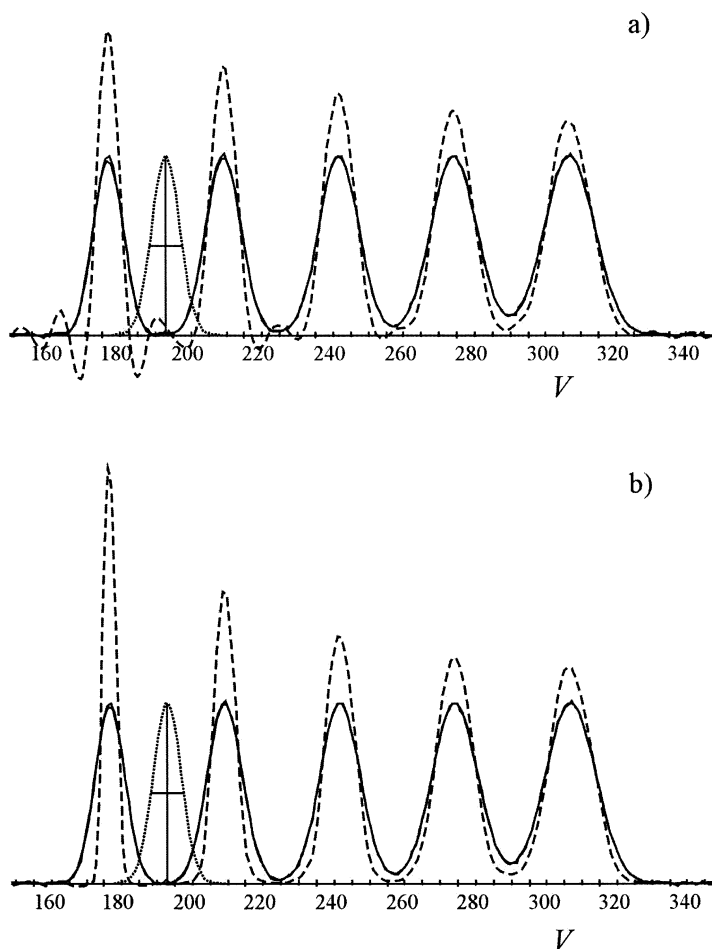
Figure 6. Numerical example for testing two inversion methods: the REG2 quadratic filter (a); and the maximum entropy method (MEM) (b). The chromatogram (in continuous trace) was produced by addition of five Gaussian distributions of an increasing width. The kernel is uniform and Gaussian, and is indicated by an internal cross. The kernel width coincides with the width of the further-left Gaussian of the chromatogram. The recuperations are shown in discontinuous trace.
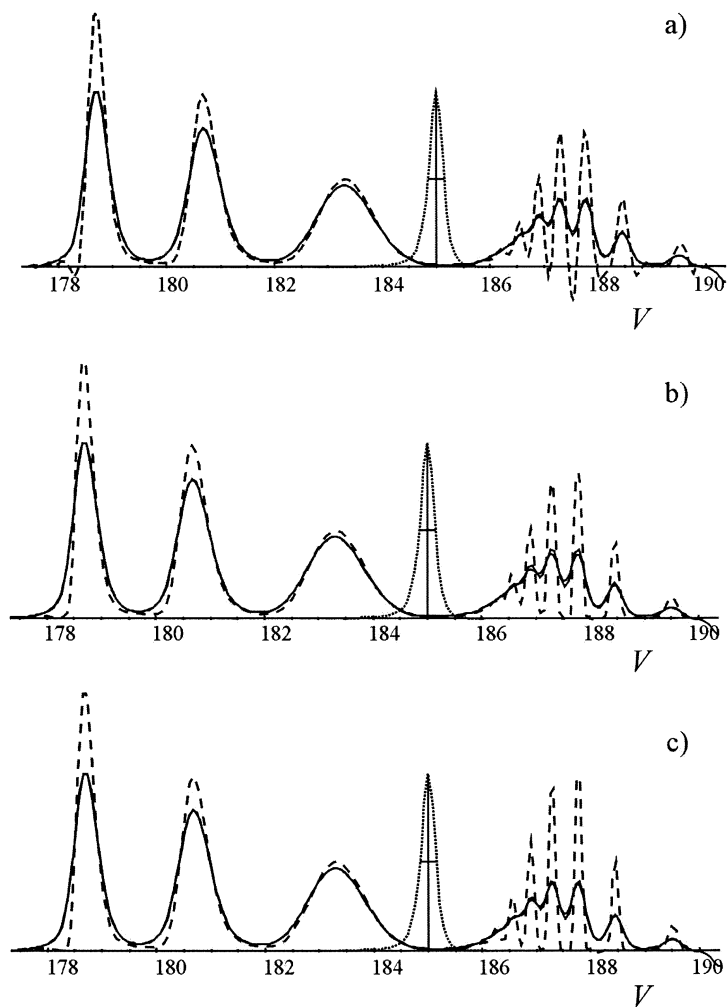
1988 BAUMGARTEN, BUSNEL, AND MEIRA

Figure 7. A chromatogram obtained by mixture of four (anionic and low-molecular-weight) standards of PMMA is deconvolved using the following techniques: global REG2 (a); global MEM (b); and local MEM (c). The low-molecular weight end is best resolved with local MEM. For chromatograms that are broader than about two times the kernel, then all three methods yield similar results. The kernel is uniform, and is indicated by an internal cross. The inversions are shown in discontinuous trace.
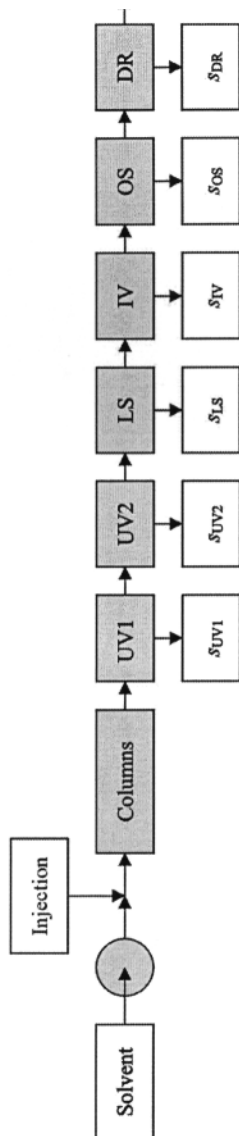
Figure 8. A case of multidetection SEC. The chromatograph is fit with: (i) two UV absorbance sensors at different wavelengths (UV1 and UV2); (ii) three molar mass sensors: a LS sensor, an (hypothetical) colligative property osmometer (OS), and a capillary IV; and (iii) a DR.

$s_{DR}(V)$, respectively. The approach that follows is quite general, and it does not enter into details of the different detector types.

The aim here is to produce unbiased estimates in multidetection SEC. Consider first, an example where both a linear and a nonlinear signal processing is required. An AB copolymer is analyzed by two UV signals: $s_{UV1}(V)$ that only responds to repeating unit A, and $s_{UV2}(V)$ that only responds to repeating unit B. To calculate the instantaneous mass $w(V)$, the following linear equation can be written:

$$w(V) = k_1 s_{UV1}(V) + k_2 s_{UV2}(V) \qquad (27)$$

where $w(V)$ is the instantaneous mass; and k_1 and k_2 are known constants. In contrast, to calculate the instantaneous mass fraction of A, $p_A(V)$, the following nonlinear combination of chromatograms is required:

$$p_A(V) = \frac{k_1 s_{UV1}(V)}{k_1 s_{UV1}(V) + k_2 s_{UV2}(V)} \qquad (28)$$

The most important case of nonlinear signal processing deals with the signal ratios associated with molar mass sensors; yielding:

$$M_w(V) = k_{LS} \frac{s_{LS}(V)}{w(V)}; \quad M_v(V) = k_{IV}\left[\frac{s_{IV(V)}}{w(V)}\right]^{1/a}$$

$$M_n(V) = k_{OS} \frac{w(V)}{s_{OS}(V)} \quad M_w(V) \geq M_v(V) \geq M_n(V) \qquad (29)$$

where $w(V)$ is the mass chromatogram.

Other nonlinearities can be stronger than the signal ratios of Eqs. (28) or (26). This is the case of estimating the number of branching points per molecule from a IV signal and the Zimm–Stockmayer relationships.[53] In this work, only the nonlinearities of Eqs. (28) and (29) will be discussed.

Consider the propagation of errors in the absence of BB, but in the presence of a measurement noise. Assume that the measured chromatograms are contaminated by additive white noises of a zero-mean and a constant variance; but that the corresponding noise-free signals are perfectly accurate. Thus, the signal-to-noise ratio is high at the chromatogram maximum, but low near to the baselines. For variables obtained by linear combination of two or more chromatograms, the propagation of errors is simple and "well-behaved". In contrast, for variables obtained from signal ratios, acceptable estimates are only feasible in the mid-chromatogram region, while "explosive" or intolerable errors are observed near to the baselines.

Now assume a perfect detection without noise, but in the presence of BB. In this case, any derived variable will also be perfectly accurate, and for this reason, global averages are, in general, unaffected by BB. Typical examples of this are: (a) the global $\overline{M}_n$ obtained from $\left\{\sum_V [w(V)/M_n(V)]\right\}^{-1}$; (b) the global $\overline{M}_w$

BAND BROADENING IN SIZE EXCLUSION CHROMATOGRAPHY   **1991**

obtained from $\sum_V M_w(V)w(V)$; and (c) the global mass fraction of A in an AB copolymer obtained from: $\bar{p}_A = \sum_V p_A(V)w(V)$.

The general method for BB correction in multidetection SEC involves first deconvoluting each of the chromatograms through Eq. (2), and then calculating the (corrected) derived variable by linear or nonlinear combination of the corrected chromatograms. Unfortunately, this method is in practice of little practical value, due to the intolerable propagation of errors that is produced in the deconvolutions and in the calculation of the derived variable. In what follows, two procedures are presented that reduce such propagation of errors. The first procedure is applicable to any linear signal processing. The second is specific to molar mass measurement.

BB Correction and Linear Signal Processing

When a quality variable is obtained by linear combination of two or more signals, then it is preferable to first calculate the quality variable from the raw chromatograms, and to then correct such (broadened) variable for BB. To prove this, consider calculating the instantaneous copolymer mass through Eq. (28). Combining Eqs. (28) and (2), one obtains:

$$w(V) = k_1 \int g(V, \tilde{V}) s_{UV1}{}^c(\tilde{V}) \, d\tilde{V} + k_2 \int g(V, \tilde{V}) s_{UV2}{}^c(\tilde{V}) \, d\tilde{V} \tag{30}$$

and therefore:

$$w(V) = \int g(V, \tilde{V})[k_1 s_{UV1}{}^c(\tilde{V}) \, d\tilde{V} + k_2 s_{UV2}{}^c(\tilde{V})] \, d\tilde{V} \tag{31}$$

$$w(V) = \int g(V, \tilde{V}) w^c(\tilde{V}) \, d\tilde{V} \tag{32}$$

Equation (32) indicates that if a variable is obtained by linear combination of the raw chromatograms, then it is broadened by the same kernel that also broadens each of the raw chromatograms. Thus, the BB-corrected function $w^c(V)$ can be obtained by first calculating $w(V)$ through Eq. (27) and then inverting Eq. (32). This procedure requires a single inversion operation, and it is, therefore, preferable to the general correction method. Unfortunately, the approach cannot be extended to variables involving a nonlinear signal processing.

To illustrate the previous ideas, consider the SEC analysis of an AB copolymer by standard dual-detection (i.e., a UV absorbance detector plus a DR). Assume that while the UV sensor "sees" only the A repeating units, the DR

responds to both repeating unit types, but with different sensitivities. The following equations can be written:[54–58]

$$s_{\text{UV}}(V) = \text{k}_{\text{UV}} p_{\text{A}}(V) w(V) \tag{33}$$

$$s_{\text{DR}}(V) = \text{k}_{\text{DR}} \{v_{\text{PA}} p_{\text{A}}(V) + v_{\text{PB}}[1 - p_{\text{A}}(V)]\} w(V) \tag{34}$$

where $w(V)$ is the instantaneous mass; $p_{\text{A}}(V)$ is the instantaneous mass fraction of A; k_{UV}, k_{DR} are the (known) UV and DR sensor gains; and v_{PA}, v_{PB} are the (known) specific refractive index increments of the poly(A) and poly(B) homopolymers. Solving for the unknowns in Eqs. (33) and (34), one finds:

$$w(V) = \left(\frac{1}{\text{k}_{\text{DR}} \, v_{\text{PB}}}\right) s_{\text{DR}}(V) + \left(\frac{v_{\text{PB}} - v_{\text{PA}}}{\text{k}_{\text{UV}} \, v_{\text{PB}}}\right) s_{\text{UV}}(V) \tag{35}$$

$$p_{\text{A}}(V) = \frac{1}{[(v_{\text{PB}} - v_{\text{PA}})/v_{\text{PB}}] + [\text{k}_{\text{UV}}/(\text{k}_{\text{DR}} v_{\text{PB}})] \, s_{\text{DR}}(V)/s_{\text{UV}}(V)} \tag{36}$$

Equation (35) is linear, and, therefore, the previously described procedure can be applied. First, obtain the broadened mass chromatogram $w(V)$ through Eq. (35), and then calculate $w^c(V)$ from Eq. (32). The previous approach cannot be extended to $p_{\text{A}}(V)$ in Eq. (36), however; and instead the general method is required. First, obtain $s_{\text{UV}}{}^c(V)$ and $s_{\text{DR}}{}^c(V)$ by inversion of the raw chromatograms. Then, obtain $p_{\text{A}}{}^c(V)$ from the "corrected" version of Eq. (36) [i.e., with $p_{\text{A}}(V)$, $s_{\text{UV}}(V)$, and $s_{\text{DR}}(V)$ substituted by $p_{\text{A}}{}^c(V)$, $s_{\text{UV}}{}^c(V)$, and $s_{\text{DR}}{}^c(V)$].

Molar Mass Detection

This section reviews a method that has been recently proposed by Vega and Meira[59] for calculating unbiased MWDs from molar mass sensors. The method is strictly applicable when the following assumptions are verified: (a) a chromatographically-simple polymer is analyzed; and (b) the molecular weight calibration obtained from (hypothetical) monodisperse standards is linear. This last requirement is not too restrictive if the analyzed sample is not too broad, and it does not contain a very high molar mass fraction. No requirements are imposed on the shapes of the MWD or the BB function.

If a chromatographically simple polymer is analyzed in an ideal chromatograph without BB, then the instantaneously eluting fraction is monodisperse in molar mass. Under this ideal condition, any perfectly accurate

molar mass sensor would provide a common measurement $M(V)$; and Eq. (29) may be written:

$$M(V) = k_{LS} \frac{s_{LS}{}^c(V)}{w^c(V)} = k_{IV}\left[\frac{s_{IV}{}^c(V)}{w^c(V)}\right]^{1/a} = k_{OS} \frac{w^c(V)}{s_{OS}{}^c(V)} \qquad (37)$$

where $w^c(V)$ is the mass chromatogram [obtained for example from $s_{DR}^c(V)$]; and k_{LS}, k_{IV}, a, and k_{OS} are all known constants. Note that $M(V)$ [or $\log M(V)$] both coincide with the unbiased molecular weight calibration that would be obtained if monodisperse standards were injected into the real chromatograph with BB. Also note, that an unbiased MWD can be obtained from $w^c(V)$ and $\log M(V)$.

Synthetic examples are ideal for investigating alternative BB correction procedures; and this is because the solutions are known a priori. The proposed correction procedure is illustrated by the numerical example that is presented in Figs. 9 and 10. The following assumptions are adopted: (i) the detectors are perfectly accurate, but the chromatograms are contaminated by white noises; and (ii) a chromatographically simple polymer is analyzed, and therefore, in the absence of BB, the instantaneous MWD in the detector cell is monodisperse. The basic raw data are: (a) the "true" or corrected mass chromatogram $w^c(V)$ of Fig. 9(a), with a range indicated by the inner arrows shown in the horizontal axis of Fig. 9(a); (b) the linear (unbiased) molecular weight calibration $\log M(V)$ of Fig. 9(c); and (c) the nonuniform and skewed IB function $g(V, \widetilde{V})$ of Fig. 9(a). The corrected LS chromatogram of Fig. 9(b) was calculated by adopting: $s_{LS}{}^c(V) \equiv 0.02[M(V)w^c(V)]$. From $w^c(V)$ and $\log M(V)$, the "true" MWD $w^c(\log M)$ of Fig. 9(d) was obtained, and the corresponding average molecular weights are presented in Table 5. The noisy "measurements" are given by $w(V)$ [Fig. 9(a)] and $s_{LS}(V)$ [Fig. 9(b)]. They were produced by first convoluting $w^c(V)$ and $s_{LS}{}^c(V)$ through Eq. (2), and then adding Gaussian white noises of zero-mean and constant variances. The final range of the measured chromatograms is given by the outer arrows shown on the horizontal axis of Fig. 9(a).

From the mass chromatogram $w(V)$ and the linear calibration, the (broadened) MWD $w(\log M)$ of Fig. 9(d) was obtained. The average molecular weights are both underestimated due to the BB skewness, while the polydispersity is overestimated (Table 5).

At each retention volume of the (noise-free) mass chromatogram, the instantaneous MWD in the detector cell was calculated by considering the contributions (at each given retention volume) of all the intervening (monodisperse) molecular species that constitute the sample, as determined by $w^c(V)$, $g(V, \widetilde{V})$, and $\log M(V)$. From the instantaneous MWDs, a noise-free $M_w(V)$ was calculated; and the corresponding $\log M_w(V)$ is represented by a smooth curve in Fig. 9(c). This ad hoc calibration is nonlinear and in general less steep than $\log M(V)$.
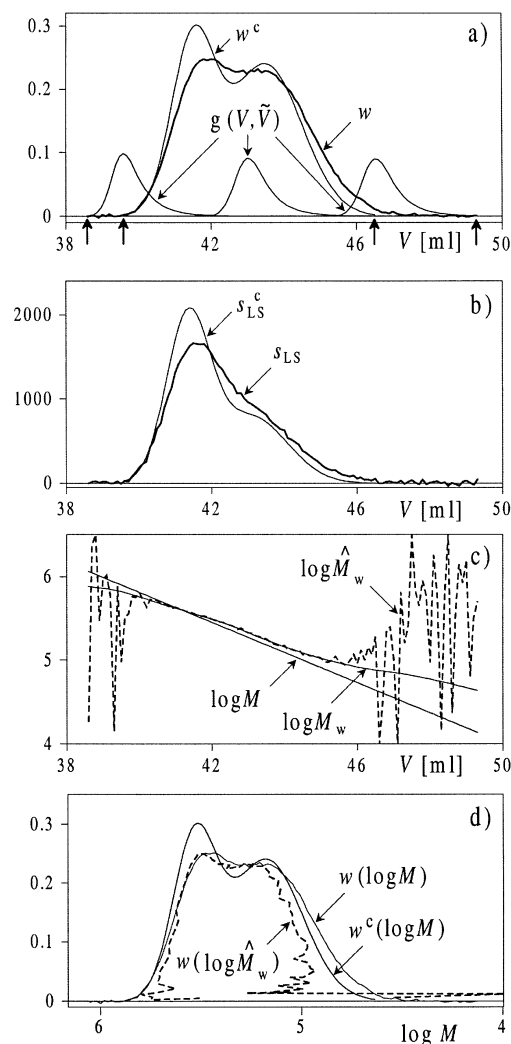
Figure 9. Simulated example of a data treatment developed for ideal LS sensors: standard procedure that does not include a correction for BB (after Vega and Meira[59]). (a) "True" mass chromatogram $w^c(V)$; three samples of the (nonuniform and skewed) spreading function, $g(V, \tilde{V})$; and measured (noisy) mass chromatogram $w(V)$. (b) "True" molar mass chromatogram $s_{LS}{}^c(V)$; and measured (noisy) molar mass chromatogram $s_{LS}(V)$. (c) Unbiased linear calibration, $\log M(V)$; "true" ad hoc calibration $\log M_w(V)$; and estimated ad hoc calibration $\log \hat{M}_w(V)$. (d) "True" MWD $w^c(\log M)$; and (unacceptable) MWD estimate $w(\log \hat{M}_w)$, directly obtained from $w(V)$ and $\log \hat{M}_w(V)$.
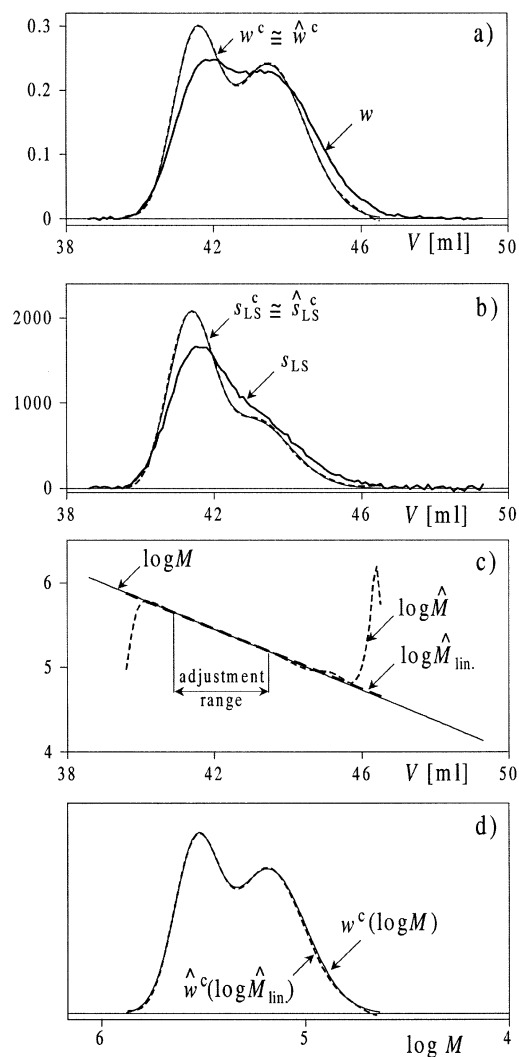
Figure 10. Simulated example of the data treatment developed for ideal LS sensors: proposed correction procedure (after Vega and Meira[59]). (a) "True" mass chromatogram $w^c(V)$; measured mass chromatogram $w(V)$; and estimated true chromatogram $\hat{w}^c(V)$. (b) "True" molar mass chromatogram $s_{LS}^c(V)$; measured molar mass chromatogram $s_{LS}(V)$; and estimated true molar mass chromatogram $\hat{s}_{LS}^c(V)$. (c) Unbiased linear calibration $\log M(V)$; estimated unbiased calibration $\log \hat{M}(V)$, and estimated linear unbiased calibration $\log \hat{M}_{lin.}(V)$. (d) "True" MWD $w^c(\log M)$ and unbiased MWD estimate $\hat{w}^c(\log \hat{M}_{lin.})$ obtained from $w^c(V)$ and $\log \hat{M}_{lin.}(V)$.

Table 5. Simulated Example of a Data Treatment Developed for an Ideal LS Sensor: Average Molecular Weights and Polydispersities

MWD	$\bar{M}_n$	$\bar{M}_w$	$\bar{M}_w/\bar{M}_n$
[a] $w^c(\log M)$ of Fig. 9(d)	182,000	242,000	1.33
[b] $w(\log M)$ of Fig. 9(d)	160,000	224,000	1.40
[c] $\hat{w}^c(\log \hat{M}_{\text{lin.}})$ of Fig. 10(d)	185,000	243,000	1.32

[a]"True" Base MWD.
[b]MWD from direct calibration and mass signal, without BB correction.
[c]Unbiased MWD from proposed correction procedure.

In a normal data treatment, $M_w(V)$ is estimated from a signals ratio, and in this example it was calculated from: $\hat{M}_w(V) = s_{\text{LS}}(V)/[0.02\,w(V)]$. The corresponding $\log \hat{M}_w(V)$ is presented in Fig. 9(c). This function is highly oscillatory at the chromatogram tails, while it almost coincides with $\log M_w(V)$ in the mid-chromatogram region. The oscillatory nature of $\log \hat{M}_w(V)$ makes it impossible to recuperate a MWD. In effect, $w(\log \hat{M}_w)$ of Fig. 9(d) is not a function at the distribution tails, and for this reason, the average molecular weights were not calculated.

The correction method is based on recuperating the unbiased (and linear) calibration $\log M(V)$ from the BB-corrected measurements. The sought calibration must only cover the expected range of the narrowed or corrected mass chromatogram $\hat{w}^c(V)$. To estimate $\log M(V)$, the following procedure is proposed: (i) correct the raw chromatograms for BB, yielding $\hat{w}^c(V)$ and $\hat{s}_{\text{LS}}{}^c(V)$; (ii) in the mid-chromatogram region, estimate the unbiased calibration from: $\hat{M}(V) = s_{\text{LS}}{}^c(V)/[0.02\,\hat{w}^c(V)]$; and (iii) adjust this last function to a straight line, and cover the range of $\hat{w}^c(V)$.

The procedure is illustrated in Fig. 10. The noisy chromatograms $w(V)$ and $s_{\text{LS}}(V)$ of Figs. 9(a,b) are reproduced in Figs. 10(a,b). These chromatograms were corrected for BB using a singular value decomposition algorithm,[38,48] and the estimates $\hat{w}^c(V)$ and $\hat{s}_{\text{LS}}{}^c(V)$ are presented in Figs. 10(a,b). Both functions are smooth, and close to the true $w^c(V)$ and $s_{\text{LS}}{}^c(V)$. The unbiased molar masses were then calculated [$\log \hat{M}(V)$ in Fig. 10(c)]. This function almost coincides with the "true" $\log M(V)$ in the mid-chromatogram region, but it diverges at the tails. Then, the linear calibration estimate $\log \hat{M}_{\text{lin.}}(V)$ was obtained from the values of $\log \hat{M}(V)$ in the "adjustment range" indicated in Fig. 10(c). Finally, the unbiased MWD $\hat{w}^c(\log \hat{M}_{\text{lin.}})$ of Fig. 10(d) was obtained from $\hat{w}^c(V)$ and $\log \hat{M}_{\text{lin.}}(V)$. The unbiased MWD almost coincides with the "true" $w^c(\log M)$; and the corresponding average molecular weights are close to the real values (Table 5). The presented procedure has not yet been tested with real experimental measurements.

CONCLUSIONS

The correction for BB in SEC is important when accurate MWDs or other polymer quality characteristics are required. In this work, the most important "state-of-the-art" problems have been reviewed and discussed.

The first task for an effective BB correction is the experimental determination of the exact broadening function or kernel for the system to be used. The sought function is generally skewed and moderately nonuniform.

Misleads in polymer quality estimates generally increase when the eluogram width becomes close to the kernel. In noise-free systems, this mislead is larger for conventional calibration than for in-line LS sensors. For samples with widths smaller than about ten times that of the kernel, equally good results are obtained via quadratic and MEM filters. For chromatogram half-widths narrower than twice the half-width of the kernel, misleads in the nonuniformity or the Mark–Houwink parameters may become dramatic. In this case, reliable results are obtained with inversion methods involving a positive solution and related filters like MEM.

In multidetection SEC, the general method for BB correction that requires the independent inversion of each of the measured chromatograms is, in general, unfeasible, due to propagation of errors in the signal processing. Two solutions have been proposed to improve that situation: one is applicable to any derived quality variable that is obtained by linear combination of chromatograms; the other is specific to molar mass sensors.

The research area is still open, and in the near future, the following advances are to be expected: (a) the development of simpler techniques for estimating the BB function, using either ultra-narrow standards or at least narrow standards with precisely-determined MWDs; (b) the experimental validation of many of the proposed numerical algorithms; (c) the inclusion (in commercial chromatographs) of software for BB correction; (d) the standardization of experimental techniques and signal processing; and (e) the commercial availability of ultra-narrow (or almost monodisperse) standards for a direct determination of the system kernel.

ACKNOWLEDGMENTS

REFERENCES

1. Berek, D.; Marcinka, K. Gel Chromatography. In *Separation Methods*; Deyl, Z., Ed.; Elsevier: Amsterdam, 1984; 271–299.

2. Hupe, K.P.; Honker, R.J.; Rozing, G. Determination of Band-Spreading Effects in High-Performance Liquid Chromatographic Instruments. J. Chromatogr. **1984**, *285*, 253–265.

3. Wyatt, P.J. Mean Square Radius of Molecules and Secondary Instrumental Broadening. J. Chromatogr. **1993**, *648*, 27–32.

4. Prougenes, P.I.; Berek, D.; Meira, G.R. Size Exclusion Chromatography of Polymers with Molar Mass Detection. Computer Simulation Study on the Biases Introduced by Instrumental Broadening and Proposed Correction Method. Polymer **1999**, *40*, 117–124.

5. Netopilik, M. Model Analysis of the Determination of the Mark–Houwink–Kuhn–Sakurada Parameters and Molecular Weight Distribution by Means of Size Exclusion Chromatography with Dual Detection. Polymer **1994**, *35*, 4799–4803.

6. Jackson, C.; Yau, W. Computer Simulation Study of Size Exclusion Chromatography with Simultaneous Viscometry and Light Scattering Measurements. J. Chromatogr. **1993**, *645*, 209–217,

7. Netopilík, M. Effect of Local Polydispersity in Size Exclusion Chromatography with Dual Detection. J. Chromatogr. A **1998**, *793*, 21–30.

8. Billiani, J.; Rois, G.; Lederer, K. A New Procedure for Simultaneous Calibration of Separation and Axial Dispersion in SEC. Chromatographia **1988**, *26*, 372–376.

9. Tung, L.H. Method of Calculating Molecular Weight Distribution Function from Gel Permeation Chromatograms. III. Application of the Method. J. Appl. Polym. Sci. **1966**, *10*, 1271–1283.

10. Tung, L.H. Method of Calculating Molecular Weight Distribution Function from Gel Permeation Chromatograms. J. Appl. Polym. Sci. **1966**, *10*, 375–383.

11. Netopilík, M. Correction for Axial Dispersion in Gel Permeation Chromatography with a Detector of Molecular Masses. Polymer Bull. **1982**, *7*, 575–582.

12. Hamielec, A.E. Correction for Axial Dispersion. In *Steric Exclusion Liquid Chromatography of Polymers*; Janca, J., Ed.; Marcel Dekker, Inc.: New York, 1984; 117–160.

13. Hamielec, A.E.; Ray, W.H. An Analytical Solution to Tung's Axial Dispersion Equation. J. Appl. Polym. Sci. **1969**, *13*, 1319–1321.

14. Balke, S.T.; Hamielec, A.E. Polymer Reactors and Molecular Weight Distribution: VIII a Method of Interpreting Skewed Chromatograms. J. Appl. Polym. Sci. **1969**, *13*, 1381–1419.

15. Netopilík, M. Analytical Solution of the Effects of Axial-Dispersion in the Analysis of a Polymer with the Log-Normal Distribution by Gel-Permeation

       Chromatography with a Molecular-Weight Detector. Polym. Bull. **1983**, *10*, 478–481.

16.   Lederer, K.; Imrich-Schwarz, G.; Dunky, M. Simultaneous Calibration of Separation and Axial-Dispersion in Size Exclusion Chromatography Coupled with Light Scattering. J. Appl. Polym. Sci. **1986**, *32*, 4751–4760.

17.   Baumgarten, J.L. Band Correction without Knowing the Kernel in SEC. A Novel Universal Method. J. Appl. Polym. Sci. **2002**, *submitted.*

18.   Duerksen, J.H.; Hamielec, A.E. Polymer Reactors and Molecular Weight Distribution: III GPC Methods of Correcting for Imperfect Resolution. J. Polym. Sci. C **1968**, *21*, 83–103.

19.   Kim, C.J.; Hamielec, A.E.; Benedek, A.J. Characterization of Nonionic Polyacrylamides by Aqueous SEC Using a DRI/LALLSP Detector System. J. Liq. Chromatogr. **1982**, *5*, 1277–1294.

20.   Billiani, J.; Amtmann, I.; Mayr, T.; Lederer, K.D. Calibration of Separation and Instrumental Peak Broadening in SEC Coupled with Light Scattering of Simple Polymers. J. Liq. Chrom. **1990**, *13*, 2973–2986.

21.   Netopilík, M. Combined Effect of Interdetector Volume and Peak Spreading in Size Exclusion Chromatography with Dual Detection. Polymer **1997**, *38*, 127–130.

22.   Jackson, C. Evaluation of the "Effective Volume Shift" Method for Axial Dispersion Corrections in Multi-Detector Size Exclusion Chromatography. Polymer **1999**, *40*, 3735–3742.

23.   Lee, H.C.; Chang, T.; Harville, S.; Mays, J.W. Characterization of Linear and Star Polystyrene by Temperature-Gradient Interaction Chromatography with a Light-Scattering Detector. Macromolecules **1998**, *31*, 690–694.

24.   Lee, H.C.; Lee, W.; Chang, T.; Yoon, J.S.; Frater, D.J.; Mays, J.W. Linking Reaction Kinetics of Star-Shaped Polystyrene by Temperature Gradient Interaction Chromatography. Macromolecules **1998**, *31*, 4114–4119.

25.   Chang, T.; Lee, H.C.; Lee, W.; Park, S.; Ko, P. Polymer Characterization by Temperature Gradient Interaction Chromatography. Macromol. Chem. Phys. **1999**, *200*, 2188–2204.

26.   Busnel, J.P.; Foucault, F.; Denis, L.; Lee, W.; Chang, T. Investigation and Interpretation of Band Broadening in Size Exclusion Chromatography. J. Chromatogr. A **2001**, *30*, 61–71.

27.   Grushka, E. Characterisation of Exponentially-Modified Gaussian Peaks in Chromatography. Anal. Chem. **1972**, *44*, 1733–1738.

28.   Lan, K.; Jorgenson, J.W. A Hybrid of Exponential and Gaussian Function as a Simple Model of Asymmetric Chromatographic Peaks. J. Chromatogr. A **2001**, *915*, 1–13.

29.   Ouano, A.C. Gel Permeation Chromatography V: Overloading Effects. J. Polym. Sci. A **1971**, *9*, 2179–2192.

30. Busnel, J.P.; Bonnans-Plaisance, C.; Retif, Ph.; Degoulet, C. Characterization of Polythiiranes Using Multidetection Size Exclusion Chromatography. J. Liq. Chromatogr. & Rel. Technol. **2001**, *24*, 921–936.

31. Provder, T.; Rosen, E.M. Instrument Spreading Correction in GPC. 1. General Shape Function Using a Linear Calibration Curve. Sepn. Sci. **1970**, *5*, 437–484.

32. Groetsch, C.W. Pitman Advanced Publishing Program. The Theory of Thikonov Regularization for Fredholm Equations of the First Kind. Boston, 1984.

33. Press, W.H.; Teukolsky, S.A.; Vetterling, W.T.; Flannery, B.P. *Numerical Recipes in C, Chapter 18: Integral Equations and Inverse Theory*; Cambridge University Press: 1996.

34. van Cittert, P.H. Z. Physik **1935**, *69*, 298.

35. Chang, K.S.; Huang, R.Y.M. A New Method for Calculating and Correcting Molecular Weight Distributions from Gel Permeation Chromatography. J. Appl. Polym. Sci. **1969**, *13*, 1459–1471.

36. Smit, J.A.M.; Hoogervorst, C.J.P.; Staverman, J.A. J. Appl. Polym. Sci. **1971**, *15*, 1479.

37. Pan, V.; Reif, J. Proceedings of the 17th Annual ACM Symp. on Theory of Computing, 1985.

38. Press, W.H.; Teukolsky, S.A.; Vetterling, W.T.; Flannery, B.P. *Numerical Recipes in C, Chapter 2.5: Iterative Improvement of a Solution to Linear Equations*; Cambridge University Press: 1996.

39. Jansson, P.A.; Hunt, R.H.; Plyler, E.K. Resolution Enhancement of Spectra. J. Opt .Soc. Am. **1970**, *60*, 596–599.

40. Press, W.H.; Teukolsky, S.A.; Vetterling, W.T.; Flannery, B.P. *Numerical Recipes in C, Chapter 10.8.: Linear Programming and the Simplex Method*; Cambridge University Press: 1996.

41. Frieden, B.R. Restoring with Maximum Likelihood and Maximum Entropy. J. Opt. Soc. Am. **1972**, *62*, 511–518.

42. Schell, A.C. Enhancing Angular Resolution of Incoherent Sources. Radio Electronic Eng. **1965**, *29*, 21–42.

43. Biraud, Y. A New Approach for Increasing Resolving Power by Data Processing. Astron. Astrophys. **1969**, *1*, 124.

44. Ishige, T.; Lee, S.-I.; Hamielec, A.E. Solution of Tung's Axial Dispersion Equation by Numerical Techniques. J. Appl. Polym. Sci. **1971**, *15*, 1607–1622.

45. Backus, G.; Gilbert, F. Uniqueness in Inversion of Inaccurate Gross Earth Data. Phyl. Trans. Roy. Soc. **1970**, *A 266*, 123–193.

46. Essenreiter, R. Diploma Thesis at University of Karlsruhe, Gephysikalisches Institut: Geophysical Deconvolution and Inversion with Neural Networks, 1996.

47. Honerkamp, J.; Weese, J. Tikhonovs Regularization Methods for Ill-Posed Problems. Continuum Mech. Thermodyn. **1990**, *2*, 17–30.

48. Mendel, J.M. Least-Squares Estimation: Singular-Value Decomposition. In *Lessons in Estimation Theory for Signal Processing, Communications, and Control*; Prentice Hall Inc.: New Jersey, 1995; Ch. 4, 44–57.

49. Morozov, V.A. *Methods for Solving Incorrectly Posed Problems*; Springer: New York, 1984.

50. Gold, B.; Rabiner, L.R. *Theory and Application of Digital Signal Processing*; Prentice Hall: Englewood Cliffs, NJ, 1975.

51. Cheung, P.; Lew, R.; Balke, S.T.; Mourey, T.H. SEC-Viscometer Detector Systems. II. Resolution Correction and Determination of Interdetector Volume. J. Appl. Pol. Sci. **1993**, *47*, 1701–1706.

52. Netopilík, M. Effect of Interdetector Peak Broadening and Volume in Size Exclusion Chromatography with Dual Viscometric-Concentration Detection. J. Chromatogr. A **1998**, *809*, 1–11.

53. Zimm, B.H.; Stockmayer, W.H. The Dimension of Chain Molecules Containing Branches and Rings. J. Chem. Phys. **1949**, *17* (12), 1301–1314.

54. Bielsa, R.O.; Meira, G.R. Linear Copolymer Analysis with Dual-Detection Size Exclusion Chromatography: Correction for Instrumental Broadening. J. Appl. Polym. Sci. **1992**, *46*, 835–845.

55. Mori, S.; Suzuki, T. Problems in Determining Compositional Heterogeneity of Copolymers by Size-Exclusion Chromatography and UV-RI Detection System. J. Liq. Chrom. **1982**, *4*, 1685–1696.

56. Kilz, P. Copolymer Analysis by LC Methods, Including Two-Dimensional Chromatography. In *Encyclopedia of Chromatography*; Cazes, J., Ed.; Marcel Dekker, Inc.: New York, 2001; 195–200.

57. Runyon, J.R.; Barnes, D.E.; Rudd, J.F.; Tung, L.H. Multiple Detectors for Molecular Weight and Composition Analysis of Copolymers by Gel Permeation Chromatography. J. Appl. Polym. Sci. **1969**, *13*, 2359–2369.

58. Adams, H.E. Composition of Butadiene-Styrene Copolymers by Gel Permeation Chromatography. Separ. Sci. **1971**, *6*, 259–273.

59. Vega, J.R.; Meira, G.R. SEC of Simple Polymers with Molar Mass Detection in Presence of Instrumental Broadening. Computer Simulation Study on the Calculation of Unbiased Molecular Weight Distributions. J. Liq. Chrom. & Rel. Technol. **2001**, *24* (7), 901–919.